THE JOURNAL OF BIOLOGICAL CHEMISTRY VOL. 284, NO. 13, pp. 8256–8264, March 27, 2009

Functional Characterization of *tlmK* Unveiling Unstable Carbinolamide Intermediates in the Tallysomycin Biosynthetic Pathway*[S]

Received for publication, January 28, 2009 Published, JBC Papers in Press, February 3, 2009, DOI 10.1074/jbc.M900640200

Liyan Wang[‡1], **Meifeng Tao**[‡1], **Evelyn Wendt-Pienkoski**[‡], **Ute Galm**[‡], **Jane M. Coughlin**[§], **and Ben Shen**[‡§¶2]

From the [‡]*Division of Pharmaceutical Sciences,* [§]*Department of Chemistry, and* [¶]*University of Wisconsin National Cooperative Drug Discovery Group, University of Wisconsin, Madison, Wisconsin 53705-2222*

Tallysomycins (TLMs) belong to the bleomycin family of anticancer antibiotics. TLMs differ from bleomycins primarily by the presence of a 4-amino-4,6-dideoxy-L-talose sugar attached to C-41 as part of a glycosylcarbinolamide. We previously proposed, on the basis of bioinformatics analysis of the *tlm* biosynthetic gene cluster from *Streptoalloteichus hindustanus* E465-94 ATCC 31158, that the *tlmK* gene is responsible for the attachment of this sugar moiety. We now report that inactivation of *tlmK* in *S. hindustanus* abolished TLM A and TLM B production, the resultant Δ*tlmK* mutant instead accumulated five new metabolites, and introduction of a functional copy of *tlmK* to the Δ*tlmK* mutant restored TLM A and TLM B production. Two major metabolites, TLM K-1 and TLM K-2, together with three minor metabolites, TLM K-3, TLM K-4, and TLM K-5, were isolated from the Δ*tlmK* mutant, and their structures were elucidated. These findings provide experimental evidence supporting the previous functional assignment of *tlmK* to encode a glycosyltransferase and unveil two carbinolamide pseudoaglycones as key intermediates in the TLM biosynthetic pathway. TlmK stabilizes the carbinolamide intermediates by glycosylating their hemiaminal hydroxyl groups, thereby protecting them from hydrolysis during TLM biosynthesis. In the absence of TlmK, the carbinolamide intermediates fragment to produce an amide TLM K-1 and aldehyde intermediates, which undergo further oxidative fragmentation to afford carboxylic acids TLM K-2, TLM K-3, TLM K-4, and TLM K-5.

Tallysomycins (TLMs)[3] belong to the bleomycin (BLM) family of glycopeptide antitumor antibiotics (1, 2) (Fig. 1). The BLMs are currently used clinically under the trade name Blenoxane® in combination with a number of other agents for the treatment of Hodgkin lymphoma, carcinomas of the skin, head, and neck, and testicular cancers. Early development of drug resistance and dose-dependent pulmonary toxicity are major limitations of BLMs in chemotherapy (3, 4). Structural modifications to this family of natural products are necessary for improvement in efficacy and reduction of toxicity. Although numerous BLM analogs have been synthesized (5, 6), total synthesis remains of limited practical value because of the complex scaffold of this entire family of natural products. Recent cloning and characterization of the BLM, TLM, and zorbamycin biosynthetic gene clusters from *Streptomyces verticillus* ATCC15003 (7), *Streptoalloteichus hindustanus* E465-94 (ATCC 31158) (8), and *Streptomyces flavoviridis* ATCC21892 (9) opened the possibility toward the production of novel BLM analogs via genetic metabolic engineering approaches.

TLMs are structurally related to BLMs but differ from BLMs in three ways; (i) the presence of two hydroxyl groups within the aminoethylbithiazole moiety, one of which is conjugated to a 4-amino-4,6-dideoxy-L-talose sugar as part of a glycosylcarbinolamide, (ii) the presence of two series of C-terminal amine moieties with (A series) or without (B series) a β-lysine moiety in the subterminal position, and (iii) the absence of a methyl group in the valerate moiety (Fig. 1). One of the B-series TLM analogs, TLM S10b, which has a 1,4-diaminobutane as the C-terminal amine moiety, exhibited antitumor activity similar to that of the BLMs in preclinical studies but failed to yield the desired response in phase II clinical trials due to poor cell penetration (10, 11). The results of preclinical and clinical studies indicate that the sugar moieties in the BLM family compounds take part in cellular recognition and drug uptake. Because one of the main differences between the BLMs and TLMs is the presence of a third sugar moiety in the TLMs, we sought to generate the des-talose TLMs to determine whether the talose moiety is responsible for the poor cell penetration of TLM S10b.

It is apparent upon comparing and contrasting the genes identified within the *tlm* and *blm* clusters that both clusters contain the genes proposed to be responsible for the synthesis and attachment of the L-gulose-3-*O*-carbamoyl-D-mannose disaccharide. At the downstream part of the *tlm* gene cluster, however, there is a *tlmHJK* operon, the homolog of which is absent in the *blm* cluster. This small operon has been proposed to be involved in the biosynthesis of the 4-amino-4,6-dideoxy-L-talose and its attachment to the TLM nonribosomal peptide skeleton. TlmK, which shows low sequence homology to known glycosyltransferases, was proposed to catalyze the attachment of the talose sugar to the aminoethylbithiazole moi-

* This work was supported, in whole or in part, by National Institutes of Health Grant CA94426.

[S] The on-line version of this article (available at http://www.jbc.org) contains supplemental Tables 1–3.

[1] Both authors were equal contributors.

[2] To whom correspondence should be addressed: 777 Highland Ave., Madison, WI 53705. Tel.: 608-263-2673; Fax: 608-262-5245; E-mail: bshen@pharmacy.wisc.edu.

[3] The abbreviations used are: TLMs, tallysomycins; BLMs, bleomycins; ^{1}H-^{1}H COSY, ^{1}H-^{1}H correlation spectroscopy; ESI, electrospray ionization; HPLC, high performance liquid chromatography; MS, mass spectroscopy; MALDI, matrix-assisted laser desorption ionization; LC, liquid chromatography.

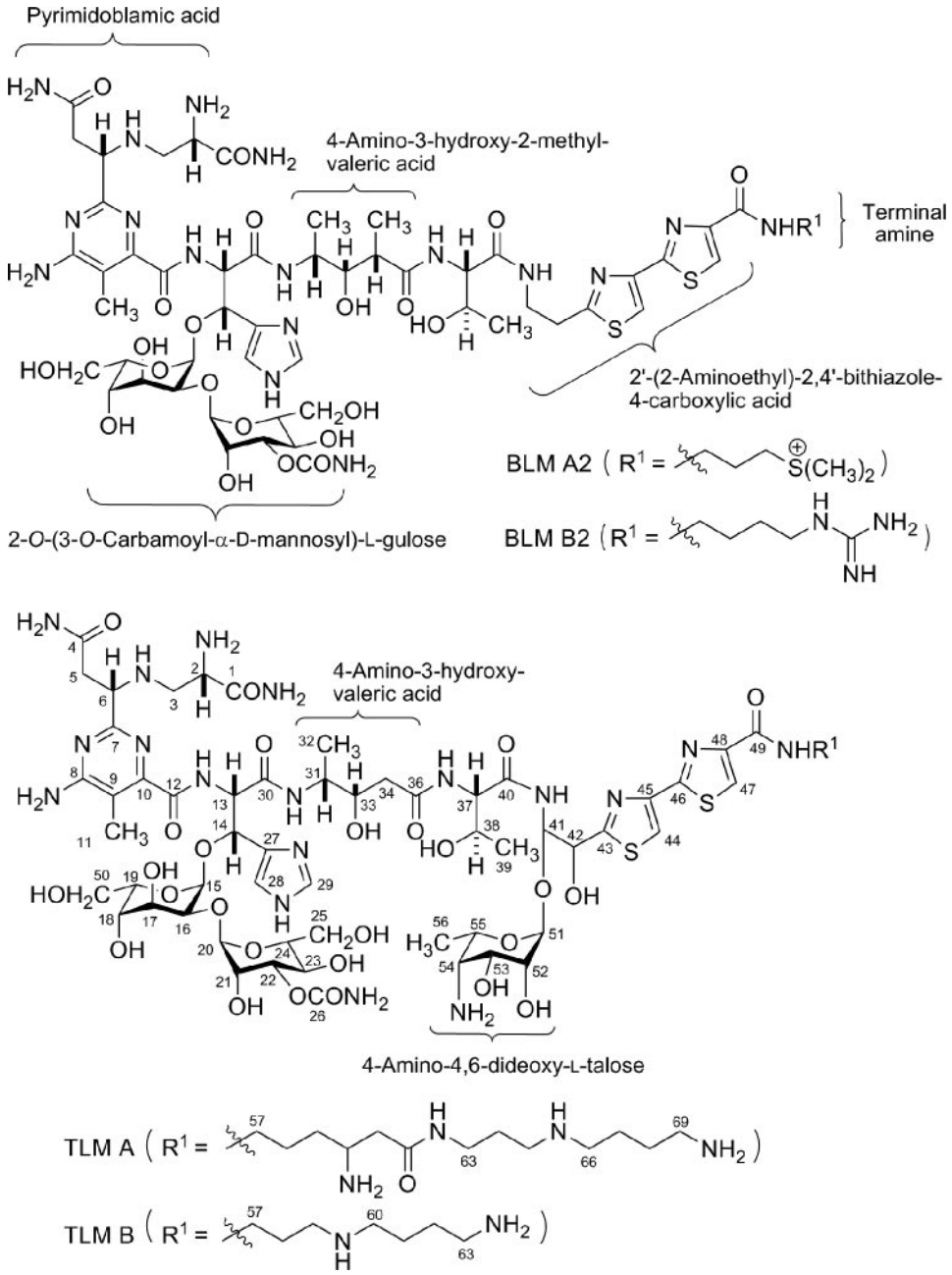

FIGURE 1. **Structures of selected members of the BLM family of antitumor antibiotics BLM A2, BLM B2, TLM A, and TLM B.**

ety (8). However, the sequence of attachments of the sugar moieties, the L-gulose-3-*O*-carbamoyl-D-mannose disaccharide and the 4-amino-4,6-dideoxy-L-talose, could not be predicted by bioinformatics analysis alone.

The aims of the present study were (i) to provide genetic proof for the role of *tlmK* in TLM biosynthesis, (ii) to determine the sequence of the sugar attachments, and (iii) to engineer TLM analogs that specifically lack the talose moiety. Here we report that inactivation of *tlmK* in *S. hindustanus* abolished TLM A and TLM B production, the resultant Δ*tlmK* mutant instead accumulated five new metabolites, and introduction of a functional copy of *tlmK* to the Δ*tlmK* mutant restored TLM A and TLM B production. Isolation and structural characterization of the five metabolites support the previous functional assignment of *tlmK* to encode a glycosyltransferase, unveil two carbinolamide pseudoaglycones as key intermediates in the TLM biosynthetic pathway, and suggest the TlmK-catalyzed glycosylation most likely occurred after the attachment of the disaccharide moiety to the TLM aglycone.

EXPERIMENTAL PROCEDURES

Bacterial Strains, Plasmids, and Culture Conditions—S. hindustanus E465-94 ATCC31158 (American Type Culture Collection, Manassas, VA) and derived recombinant strains were routinely cultivated at 30 °C on ISP4 agar medium supplemented with $MgCl_2$ to final concentration of 28 mM or TSB liquid medium. *Escherichia coli* DH5α and ET12567 (12) were grown in liquid or on solid Luria-Bertani medium at 37 °C (13). *E. coli* BW25113/pIJ790 and BT340 were cultivated according to the λ RED-mediated PCR-targeting mutagenesis kit (14). Electroporation using *S. hindustanus* spores was carried out as previously described (8).

pIJ780 from the λ RED-mediated PCR-targeting mutagenesis kit (14) was modified by replacing the viomycin resistance gene (*vph*) with the kanamycin-neomycin resistance gene (*neo*) from Supercos1 (Stratagene, La Jolla, CA) to yield pBS8010. pBS8010 was then used as template to amplify the FRT-*neo* cassette for replacing *tlmK* in pBS8008 (8) following the λ RED-mediated PCR-targeting mutagenesis protocol. Cosmid pBS8008 carrying 41.6-kilobase *S. hindustanus* genomic DNA encoding part of the *tlm* biosynthetic gene cluster was used to construct the gene deletion mutant allele in *E. coli* by the λ RED-mediated PCR-targeting mutagenesis method. The *aac(3)IV-tsr* apramycin and thiostrepton resistance gene cassette in its vector backbone was used for selection in both *E. coli* and *S. hindustanus*. pBS8004 (8) carrying the Φ*C31* integration function region and the thiostrepton resistance marker *tsr* were used to construct the *tlmK* expression plasmid (supplemental Tables S1 and S2).

Construction of the Δ*tlmK In-frame Deletion Mutant Strain SB8003*—The Δ*tlmK* in-frame deletion mutant was constructed via a homologous recombination strategy. First, a *tlmK* allele in pBS1011 was constructed in *E. coli* by the λ RED-me-

diated PCR-targeting mutagenesis strategy from pBS8008 using oligonucleotides tlmK-frt1 and tlmK-frt2 (supplemental Table S3). This replaced the *tlmK* gene in pBS8008 with the FRT-*neo* cassette amplified from pBS8010 to afford pBS8011. Next, the FRT-*neo* cassette of pBS8011 was removed by the FLP recombination function provided by *E. coli* BT340 according to the instructions of the λ RED-mediated PCR-targeting mutagenesis kit (14). In the resulting cosmid pBS8012, the entire *tlmK* open reading frame was deleted, leaving only the ATG start codon, the TGA stop codon, and an 81-bp stretch of unrelated nucleotides between the ATG and TGA codons. Finally, pBS8012 was passed through *E. coli* ET12567 to produce demethylated plasmid DNA and subsequently transferred into *S. hindustanus* wild-type strain by electroporation. Thiostrepton-resistant transformants were selected and underwent one round of nonselective sporulating growth; resulting spores were plated out and screened for thiostrepton-sensitive colonies.

The genotype of these thiostrepton-sensitive isolates was determined by PCR using primers tlmK-up and tlmK-down (supplemental Table S3), resulting in identification of five Δ*tlmk* in-frame deletion mutant isolates named SB8003. The genotype of SB8003 was further confirmed by Southern hybridization using the 2238-bp fragment amplified by PCR with primers tlmK-up and tlmK-down (supplemental Table S3) from the *S. hindustanus* wild-type genomic DNA as a probe. DNA isolations and manipulations were carried out according to standard protocols (13, 15). Southern hybridization using digoxigenin-labeled DNA probes was performed according to manufacturer provided protocols (Roche Diagnostics).

*Genetic Complementation of the Δ*tlmK* In-frame Deletion Mutant Strain SB8003*—The *ErmE** promoter was amplified from pWHM79 by PCR using primers PermEI-f and PermEI-r (supplemental Table S3) and cloned as an EcoRI-BamHI fragment into the same sites of pBS8004 to yield the integrative vector pBS8013. The *tlmK* gene was amplified from pBS8008 using primers tlmK-NsiI and tlmK-XbaI (Table S3) and cloned as an NsiI-XbaI fragment into the same sites of pBS8013 to afford pBS8014. pBS8014 was introduced into SB8003 by electroporation, and selection with thiostrepton resistance afforded the Δ*tlmK*-complemented recombinant strain SB8004.

Production, Isolation, and Analyses of TLM A, B, K-1, K-2, K-3, K-4, and K-5—The *S. hindustanus* wild-type strain, the Δ*tlmK* mutant strain SB8003, and the Δ*tlmK*-complemented recombinant strain SB8004 were cultured in 50 ml of production medium as described previously (8). After centrifugation, the supernatant (~40 ml) was adjusted to pH 7.0 with 1.0 M HCl and mixed with Amberlite® IRC50 resin (H^+-type, 10 ml). After incubation of the resultant slurry at room temperature with gentle agitation for 30 min, the Amberlite® IRC-50 resin was packed into a column, washed with 10 bed-volumes of water, and drained of excess water. TLM A and B from the wild-type ATCC 31158 and the recombinant SB8004 strains and TLM K-1, K-2, K-3, K-4, and K-5 from the Δ*tlmK* mutant SB8003 strain were eluted with 30 ml of 0.2 M HCl. The Amberlite® IRC50 eluent was neutralized with 1.0 N NaOH and concentrated *in vacuo* to ~1 ml. Analytic HPLC was carried out on an Apollo C-18 column (5 μm, 250 × 4.6 mm, Alltech Associates, Inc., Deerfield, IL). The column was equilibrated with 100% solvent A (99.8% H_2O, 0.2% acetic acid) and 0% solvent B (99.8% methanol, 0.2% acetic acid) and developed with a linear gradient (0–5 min, linear gradient from 100% A/0% B to 90% A/10% B; 5–30 min, linear gradient from 90%A/10% B to 0% A/100% B; 30–35 min, 0% A/100% B) at a flow rate of 0.7 ml/min and UV detection at 300 nm using a Varian Prostar 330 PDA detector (Varian, Palo Alto, CA). Under these conditions, TLM A and B were eluted with retention time of 11.0 and 12.4 min, respectively, whereas TLM K-1, K-2, K-3, K-4, and K-5 were eluted with retention time of 10.4, 15.2, 15.8, 16.3, and 16.9 min, respectively.

For preparative-scale isolation of the TLM K-1, K-2, K-3, K-4, and K-5 from the Δ*tlmK* mutant SB8003 strain, the fermentation culture (10 liters) was centrifuged at 3000 rpm for 30 min, and the supernatant was collected, adjusted to pH 7.0 with 1.0 M HCl, and loaded onto an Amberlite® XAD-16 column (1.0 liter). After washing the column with three bed volumes of H_2O, these intermediates were eluted with 2.0 liters of 80% MeOH. The resulting eluent was concentrated *in vacuo* to ~10 ml and then loaded to a CM-Sephadex C-25 (50 × 20 mm) column. The column was washed with 3 bed-volumes of H_2O and eluted with 0.1, 0.2, 0.3, 0.5, or 1.0 M NH_4OAc sequentially. Fractions containing TLM K-1 were eluted at 0.1 M NH_4OAc, fractions containing TLM K-4 and K-5 were eluted at 0.2 M NH_4OAc, fractions containing TLM K-2 were eluted at 0.3 M NH_4OAc, and fractions containing TLM K-3 were eluted at 0.5 M NH_4OAC. Fractions containing each metabolite were re-loaded onto Amberlite® XAD-16 columns (50 × 20 mm). The columns were washed with three bed-volumes of H_2O and then eluted with three bed-volumes of 80% MeOH. The MeOH eluents were then concentrated *in vacuo* to ~2 ml.

Final purification of each metabolite was achieved by semi-preparative HPLC on an Altima C18 column (5 μm, 250 × 10 mm, Alltech Associates, Inc.). HPLC was carried out under the following conditions. Instrument and detector were the same as stated above. The column was equilibrated with 100% solvent A (0.1% formic acid) and 0% solvent B (methanol) and developed with a linear gradient (0–15 min, from 95% A/5% B to 50% A/50% B; 15 to 18 min, from 50% A/50% B to 0% A/100% B) at a flow rate of 3 ml/min and with UV detection at 300 nm. TLM K-1, K-2, K-3, and K-5 were eluted with retention times of 5.0, 7.5, 7.7, and 8.5 min, respectively. Upon final removal of MeOH by concentration *in vacuo*, the residues were lyophilized to afford the final pure metabolites TLM K-1 (as copper complex, 4.1 mg), TLM K-2 (1.4 mg), TLM K-3 (0.5 mg), and TLM K-5 (0.3 mg), respectively. Final treatment of the TLM K-1 copper complex with 0.5 M EDTA-Na (pH 7.3) solution followed by a HPLC purification step afforded copper-free TLM K-1 (3.2 mg) (8, 9).

Each of the purified metabolites was subjected to MS, one-dimensional and two-dimensional ^1H or ^{13}C NMR spectroscopic analyses, or a combination of thereof for structural determination. LC-MS analysis was carried out on an Agilent 1100 HPLC-MSD SL quadrupole mass spectrometer (Santa Clara, CA), and high resolution matrix-assisted laser desorption ionization (MALDI)-Fourier transform MS analysis was

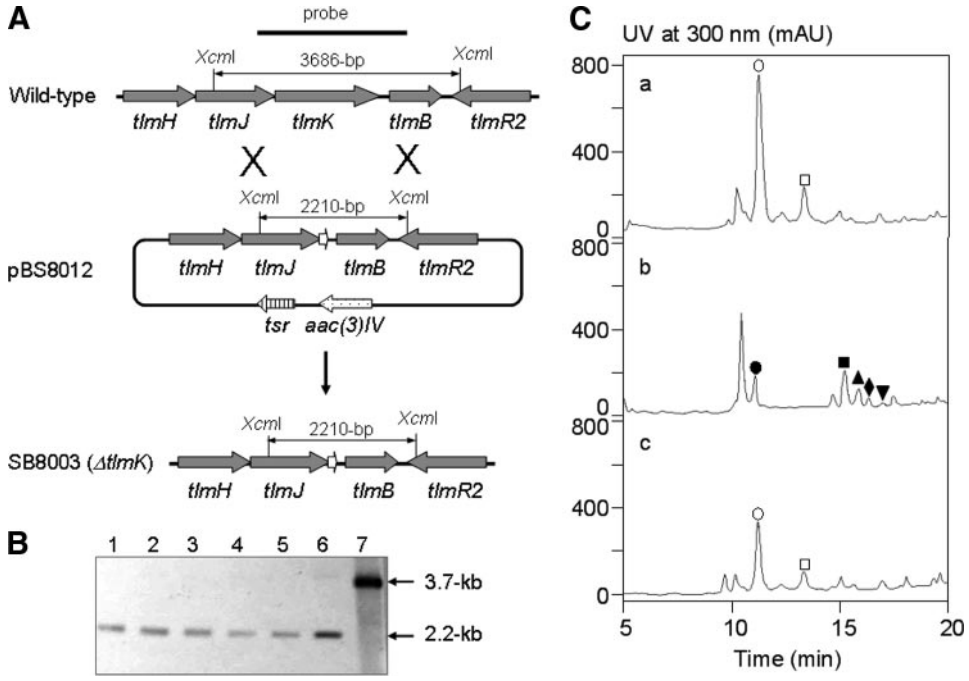

FIGURE 2. **Inactivation of *tlmK* and genetic complementation to the Δ*tlmK* in-frame deletion mutant.** *A*, construction of the Δ*tlmK* mutant strain SB8003 and restriction maps of the *S. hindustanus* wild-type and SB8003 mutant strains as well as the pBS8012 cosmid carrying the Δ*tlmK* in-frame deletion mutation upon XcmI digestion. *B*, Southern analysis of the Δ*tlmK* mutant strain SB8003 (*lanes 1*, *2*, *3*, *4*, and *5* for five independent isolates) with the Δ*tlmK* mutant construct pBS8012 (*lane 6*) and *tlmK* wild-type construct pBS8008 (*lane 7*) as controls upon XcmI digestion and using the 2.2-kilobase (*kb*) PCR-amplified fragment from the wild-type strain as a probe. *C*, HPLC analysis of (*a*) TLM production in *S. hindustanus* wild type, (*b*) new metabolite accumulation in the Δ*tlmK* mutant strain SB8003, and (*c*) restoration of TLM production in the Δ*tlmK*-complemented recombinant strain SB8004. ○, TLM A; □, TLM B; ●, TLM K-1; ■, TLM K-2; ▲, TLM K-3; ◆, TLM K-4; ▼, TLM K-5. *mAU*, milliabsorbance.

carried out on an IonSpec HiResMALDI Fourier transform mass spectrometer with a 7-tesla superconducting magnet (Lake Forest, CA). ^{1}H and ^{13}C NMR spectra were obtained on a Varian Unity Inova 500 instrument at 500 MHz for ^{1}H and 125 MHz for ^{13}C nuclei, and two-dimensional NMR spectra were performed using standard Varian pulse sequences (Palo Alto, CA).

RESULTS

Characterization of tlmK by Gene Inactivation and Mutant Complementation—To investigate its role in TLM biosynthesis, an in-frame deletion of the *tlmK* gene was generated in the TLM producing *S. hindustanus* wild-type strain by homologous recombination (Fig. 2*A*). pBS8012, carrying a Δ*tlmK* in-frame deletion mutant allele, was made from pBS8008, a cosmid carrying 41.6 kilobases of downstream part of the *tlm* gene cluster. pBS8012 was then transformed into *S. hindustanus* wild-type strain by electroporation followed by screening for double crossover homologous recombination events, yielding five isolates of the mutant strain SB8003; the Δ*tlmK* in-frame deletion genotype in SB8003 was confirmed by Southern hybridization (Fig. 2*B*). Fermentations of SB8003 showed that (i) TLM A and B production has been abolished and, (ii) instead, five new metabolites were found with retention times of 10.4 (TLM K-1), 15.2 (TLM K-2), 15.8 (TLM K-3), 16.3 (TLM K-4), and 16.9 (TLM K-5) min, which were apparently different from those of TLM A and B (Fig. 2*C*).

To genetically complement the Δ*tlmK* mutation in SB8003, pBS8014, an integrative plasmid carrying a functional copy of *tlmK*, whose expression is under control of the constitutive *ErmE** promoter (16), was conjugated into SB8003 to yield the complementation strain SB8004 (*i.e.* SB8003 (pBS8014)). The production of TLM A and B was partially restored in SB8004 with TLM A and B titers of 8–10 mg/liter, which is ~50% that for the *S. hindustanus* wild-type strain (Fig. 2*C*).

*Isolation and Structural Characterization of the New Metabolites Accumulated in the Δ*tlmK* Mutant Strain SB8003*—Deletion of *tlmK*, thereby inactivating the TlmK glycosyltransferase in TLM biosynthesis, might lead to the production of a carbinolamide intermediate lacking the talose moiety at C-41 (Fig. 1). Such intermediates may readily undergo fragmentation to afford an amide and aldehyde (see Fig. 4). As anticipated, one of the five new metabolites accumulated by SB8003 showed a $[M+Cu-H]^+$ ion at *m*/*z* 1122.3 upon LC-ESI-MS analysis, corresponding to the calculated molecular weight of the amide species TLM K-1. The other metabolites showed $[M+H]^+$ ions at *m*/*z* 542.2, 468.0, 370.1, and 340.1 upon LC-ESI-MS analysis, but none of them matched the molecular weight of the proposed aldehyde species. Instead, the ions at *m*/*z* 542.2 (TLM K-2) and 370.1 (TLM K-4) matched those of carboxylic acids oxidized from the predicted aldehydes, whereas the ions at *m*/*z* 468.0 (TLM K-3) and 340.1 (TLM K-5) matched the further decomposed products of TLM K-2 and TLM K-4, respectively. The estimated yields of TLM K-1, K-2, K-3, K-4, and K-5 are ~5.0, 3.0, 1.0, 0.5, and 0.3 mg/liter, respectively.

To establish the structures, these metabolites were isolated from large scale fermentation (10 liter). TLM K-1 was isolated as a blue powder, which is characteristic for members of the BLM and TLM family as a copper complex. To remove copper for NMR analysis, the complex was treated with EDTA to afford copper-free TLM K-1 as a pale white powder. The high resolution MALDI- Fourier transform mass spectrometry analysis of copper-free TLM K-1 yielded a $[M+H]^+$ ion at *m*/*z* 1061.4496, which corresponded to the molecular formula $C_{40}H_{64}N_{14}O_{20} + H^+$ (calculated 1061.4499). The ^{1}H and ^{13}C NMR data of copper-free TLM K-1 were almost identical to those of the left portion of TLM A, including the pyrimidoblamic acid, β-hydroxyhistidine, 4-amino-3-hydroxy pentanoic acid, threonine, and 2-*O*-(3-*O*-carbamoyl-α-D-mannosyl)-L-gulose moieties but lacked the signals corresponding to the right portion of TLM A, including the 2′-(2-amino-1,2-

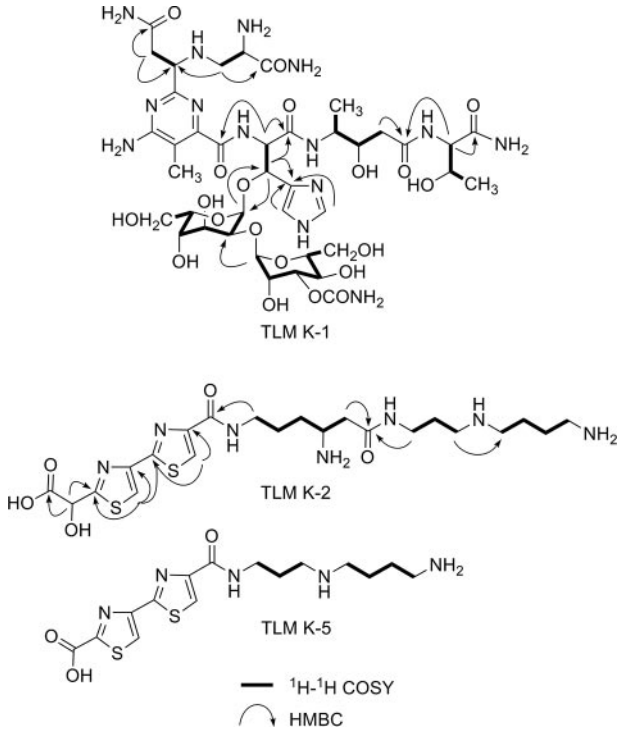

FIGURE 3. **Key ^{1}H-^{1}H COSY and heteronuclear multiple bond correlation (HMBC) correlations of TLM K-1, K-2, and K-5.**

dihydroxyethyl)-2,4′-bithiazole-4-carboxylic acid, terminal amines (for both A- and B-series of TLMs), and the 4-amino-4,6-dideoxy-L-talose moiety (17, 18) (Figs. 1 and 4). The structure of TLM K-1 was finally unambiguously determined by careful analysis of ^{1}H, ^{13}C, and two-dimensional NMR measurements as the degraded product, containing the "left" structure units mentioned above, of the proposed carbinolamide intermediates in the TLM biosynthetic pathway (Fig. 3 and Table 1).

TLM K-2, K-3, and K-5 were all purified as pale white powders. Although upon ESI-MS analysis TLM K-2 showed a $[M+H]^+$ ion at m/z 542.2, high resolution MALDI Fourier transform MS analysis of TLM K-2 afforded a decarboxylation fragment $[M\text{-}COOH+H]^+$ ion at m/z 498.2355, which agrees well with the molecular formula of $C_{21}H_{36}N_7O_3S_2 + H^+$ (calculated 498.2394). The ^{1}H and ^{13}C NMR data of TLM K-2 are almost identical to those of the "right" portion of TLM A (17, 18) (Fig. 3 and Table 2). However, an oxygen-bearing methine signal (δ_C 83.3) for C-41 observed in the ^{13}C NMR spectrum of TLM A was absent in that of TLM K-2, and instead, a new carbonyl signal at δ_C 178.0 was observed. Combined with the decarboxylation fragment detected in the MALDI-MS spectrum of TLM K-2, this carbonyl moiety was considered as a part of a newly formed carboxylic acid group. The correlation between H-42 (δ_H 5.38 s) and the carbonyl carbon indicated that this carboxylic acid group is located at C-41 (Fig. 3). On the basis of these data the complete structure of TLM K-2 was established. The structure of TLM K-2 indicates that the nascent aldehyde species (*right portion*), generated upon hydrolysis of the proposed carbinolamide intermediate, is further oxidized spontaneously to form the corresponding carboxylic acid TLM K-2 (Fig. 4).

TABLE 1

^{13}C NMR and ^{1}H NMR data of TLM K-1 [D_2O, 3-trimethylsilyl[2,2,3,3-$^2H_4$]propionate, δ (ppm) (J = HZ)]

Assignment was confirmed by ^{1}H-^{1}H COSY, total correlation spectroscopy, heteronuclear single quantum coherence, and heteronuclear multiple bond correlation spectra obtained at 500 and 125 MHz.

No.[a]	δ_C	δ_H
1	173.8	
2	55.2	4.02 m[b]
3	49.8	2.97 dd (13.5, 7.0), 3.01 dd (13.5, 5.5)
4	179.0	
5	43.0	2.66 dd (15.0, 8.5), 2.71 dd (15.0, 3.0)
6	62.8	4.00 m[b]
7	161.1	
8	167.3	
9	114.3	
10	156.2	
11	13.7	1.93 s
12	170.8	
13	59.0	5.11 d (7.5)
14	75.3	5.39 d (7.5)
15	101.6	5.28 d (4.0)
16	70.5	3.98 m[b]
17	71.9	3.88 m[b]
18	70.3	4.16 m[b]
19	72.9	4.06 m[b]
20	100.9	5.03 d (2.0)
21	71.2	4.13 m[b]
22	77.3	4.80 m[b]
23	67.6	3.85 m[b]
24	76.3	3.84 m[b]
25	63.8	3.82 m[b], 3.96 m[b]
26	161.1	
27	134.2	
28	121.6	7.54 s
29	138.4	8.53 s
30	171.5	
31	52.7	3.90 m[b]
32	17.1	1.18 d (6.5)
33	73.6	4.1 m[b]
34	42.6	2.45 dd (14.5, 9.5), 2.50 dd (14.5, 3.0)
36	177.2	
37	61.6	4.31 d (3.5)
38	69.9	4.26 m
39	21.7	1.19 d (6.5)
40	177.8	
50	63.3	3.39 dd (11.5, 7.5), 3.54 dd (11.5, 4.5)

[a] H and C numbering is based on TLM A.
[b] Overlapped signal.

ESI-MS analysis of TLM K-3 yielded $[M+H]^+$ ion at m/z 512.3, which was 30 units less (CH_2O) than that of TLM K-2. The ^{1}H NMR data of TLM K-3 are almost identical to those of TLM K-2 except for the absence of the oxygenated methine signal at δ_H 5.38 (H-42) (Table 2). The structure of TLM K-3 was then established to be a further degradation product of TLM K-2 resulting from the loss of C-41 via decarboxylation and subsequent C-42 oxidation to finally form a new carboxylic acid (Fig. 4).

LC-ESI-MS analyses of TLM K-4 and TLM K-5 afforded $[M+H]^+$ ions at m/z 414.2 and 384.2, both 128 units (equal to a β-lysine moiety) smaller than that of TLM K-2 and K-3, respectively. TLM K-4 and K-5 were, thus, considered to be breakdown products of the right portion of the carbinolamide intermediate for TLM B. An attempt to purify TLM K-4 was not successful due to its rapid conversion into TLM K-5, and the structure of TLM K-4 was, therefore, assigned on the basis of MS data and its specific conversion to TLM K-5, which was further characterized by ^{1}H NMR. Thus, the ^{1}H NMR spectrum of TLM K-5 revealed two olefin signals in the low field and seven methylene signals in the high field (Table 2). The two olefin singlets, δ_H 8.21 and δ_H 8.30, were assigned as H-44 and H-47 by comparing with those of TLM K-2 and K-3. The seven

TABLE 2

^{13}C NMR and ^{1}H NMR data of 2, 3, and 5 [D_2O, 3-trimethylsilyl[2,2,3,3-$^{2}H_4$]propionate, δ(ppm) (*J* = HZ)]

No.[c]	TLM K-2[a]		TLM K-3[a]		TLM K-5[b] δ_H
	δ_C	δ_H	δ_C	δ_H	
41	178.0		—[d]		
42	75.2	5.38 s	—		
43	175.9		—		
44	149.9	8.18 s	—	8.24 s	8.21 s
45	165.7		—		
46	165.7		—		
47	151.6	8.21 s	—	8.32 s	8.30 s
48	166.0		—		
49	172.1		—		
57	41.47	3.47 m	41.47	3.49 m	3.45 t (6.0)
58	27.3	1.75 m[e]	27.3	1.75 m[e]	2.08 m
59	32.0	1.77 m[e]	32.0	1.77 m[e]	3.20 t (6.5)
60	51.3	3.66 m	51.3	3.68 m	1.82 m[e]
61	39.4	2.63 m	39.4	2.67 m	3.17 m
62	174.7		—		1.82 m[e]
63	38.9	3.14 m	38.9	3.17 m	3.08 t (6.5)
64	28.1	1.80 m[e]	28.1	1.80 m[e]	
65	47.9	2.90 t (8.0)	47.9	2.91 t (8.0)	
66	49.7	2.98 m[e]	49.7	3.00 m[e]	
67	25.5	1.71 m[e]	25.5	1.71 m[e]	
68	26.7	1.69 m[e]	26.7	1.69 m[e]	
69	41.53	3.00 m[e]	41.53	3.02 m[e]	

[a] Assignment confirmed by ^{1}H-^{1}H COSY, total correlation spectroscopy, heteronuclear single quantum coherence, and heteronuclear multiple bond correlation spectra obtained at 500 MHz and 125 MHz.
[b] Assignment confirmed by ^{1}H NMR and ^{1}H-^{1}H COSY obtained at 500 MHz.
[c] H and C numbering is based on TLM A and TLM B.
[d] Not assigned.
[e] Overlapped signal.

methylene signals were assigned by the analyses of the ^{1}H-^{1}H COSY spectrum (Fig. 3).

DISCUSSION

The BLMs and TLMs are a family of structurally related glycopeptide-derived antibiotics with significant anti-tumor activity. The BLMs are the only members of this family that are currently used clinically in combination chemotherapy for the treatment of several types of tumors. The total chemical synthesis is of limited practical value for developing new analogs given the structural complexity of the BLM family of natural products. In contrast, a series of BLM and TLM derivatives, which differ in their terminal amines, have been produced by precursor amine feeding fermentations (19, 20). Peplomycin, which is a BLM-type compound produced by feeding with *N*-(3-aminopropyl)-α-phenylethylamine, showed lower pulmonary toxicity than the clinically used Blenoxane® and has been successfully developed as the second generation of BLMs in Japan (21). These early studies clearly demonstrated that minor structural modification in BLM-type compounds could result in significant therapeutic gains. Inspired by these findings, we sought to generate new analogs of the BLM family using combinatorial biosynthesis strategies. During our ongoing research on hybrid peptide-polyketide natural product biosynthesis, we have cloned and sequenced the gene clusters for BLM from *S. verticillus* ATCC15003 (7), TLM from *S. hindustanus* E465-94 ATCC31158 (8), and zorbamycin from *S. flavoviridis* ATCC21892 (9). This enabled us to find the differences in BLM, TLM, and zorbamycin biosynthesis and to formulate hypothesis for generating new BLM analogs by genetic manipulation of the BLM, TLM, and zorbamycin biosynthetic machineries.

Functional characterization of *tlmK* by gene inactivation followed by structural characterization of the accumulated metabolites unveiled unstable carbinolamide pseudoaglycones as key intermediates, shedding new insights into TLM biosynthesis. The *tlmK* gene, residing within the *tlmHJK* operon that is located near the downstream end of the *tlm* biosynthetic gene cluster, encodes a 520-amino acid protein (8). The C-terminal portion of TlmK exhibits low similarity (27% identity and 42% similarity) to the dihydrostreptosyl glycosyltransferase (StrH) from the streptomycin gene cluster of *Streptomyces griseus* (22). Unlike many other genes in the TLM cluster, *tlmK* has no counterpart in the *blm* biosynthetic gene cluster. Given the fact that BLMs lack the 4-amino-4,6-dideoxy-L-talose moiety, *tlmK* has been proposed to be involved in the attachment of this extra sugar moiety to the TLM aglycone (8).

Because of the unique structure of the carbinolamide where the talose sugar is attached to the TLMs, the des-talose TLMs (*i.e.* the carbinolamide pseudoaglycones) generated upon inactivation of *tlmK* might not be stable. Indeed, extensive analysis of fermentation culture of the Δ*tlmK* mutant strain SB8003 failed to detect the intact carbinolamide intermediates predicted for TLM biosynthesis. Instead, we found five new metabolites, TLM K-1, K-2, K-3, K-4, and K-5, from SB8003 and their structures established by MS and NMR analyses. These metabolites can be best interpreted as degradation products of the predicted carbinolamide intermediates (Fig. 4). Thus, the C-41 of carbinolamides first hydrolytically fragments to afford the amide TLM K-1 and aldehydes. The aldehyde species then undergo oxidation to carboxylic acids TLM K-2 and K-4, which are finally decarboxylated and oxidized at C-42 to form TLM K-3 and K-5, respectively. Although we were unable to detect the des-talose TLM directly, accumulation of these metabolites in SB8003 and their subsequent isolation and structural elucidation indirectly but unambiguously establish the function of TlmK as the glycosyltransferase responsible for the attachment of the talose sugar to the pseudoaglycone as the final step of the TLM biosynthetic pathway. In addition, isolation and characterization of TLM K-1 as the left portion of TLM containing the L-gulose-3-*O*-carbamoyl-D-mannose disaccharide moiety suggests that the attachment of this disaccharide moiety most likely occurs before the dihydroxylation and subsequent glycosylation at the aminoethylbithiazole moiety (Fig. 4) (7–9).

Although hemiaminals are in general not stable under aqueous conditions, a few carbinolamide-bearing natural products have been identified, such as the echinocandin type anti-fungal antibiotics anidulafungin (known as Eraxis®) (23) and micafungin (known as Mycamine®) (24), spergualin (25), zampanolide (26), bicyclomycin (Bicozamycin®) (27–29), epolactaene (30), and oteromycin (31) (Fig. 5). Anidulafungin is reported to chemically decompose in the normal human plasma (32, 33). Experimental evidence demonstrates in a zampanolide model compound that an intramolecular H-bond network stabilizes the hemiaminal functionality (34). Because the carbinolamide pseudoaglycones are not stable, we propose that the TlmK-catalyzed glycosylation is sufficiently fast so as to avoid hydrolytic decomposition.

DNA cleavage activities of the breakdown products provide new insights into the structural and activity relationship for the BLM family of antitumor antibiotics. The clinic effect of BLM family antibiotics is thought to be derived from their ability to

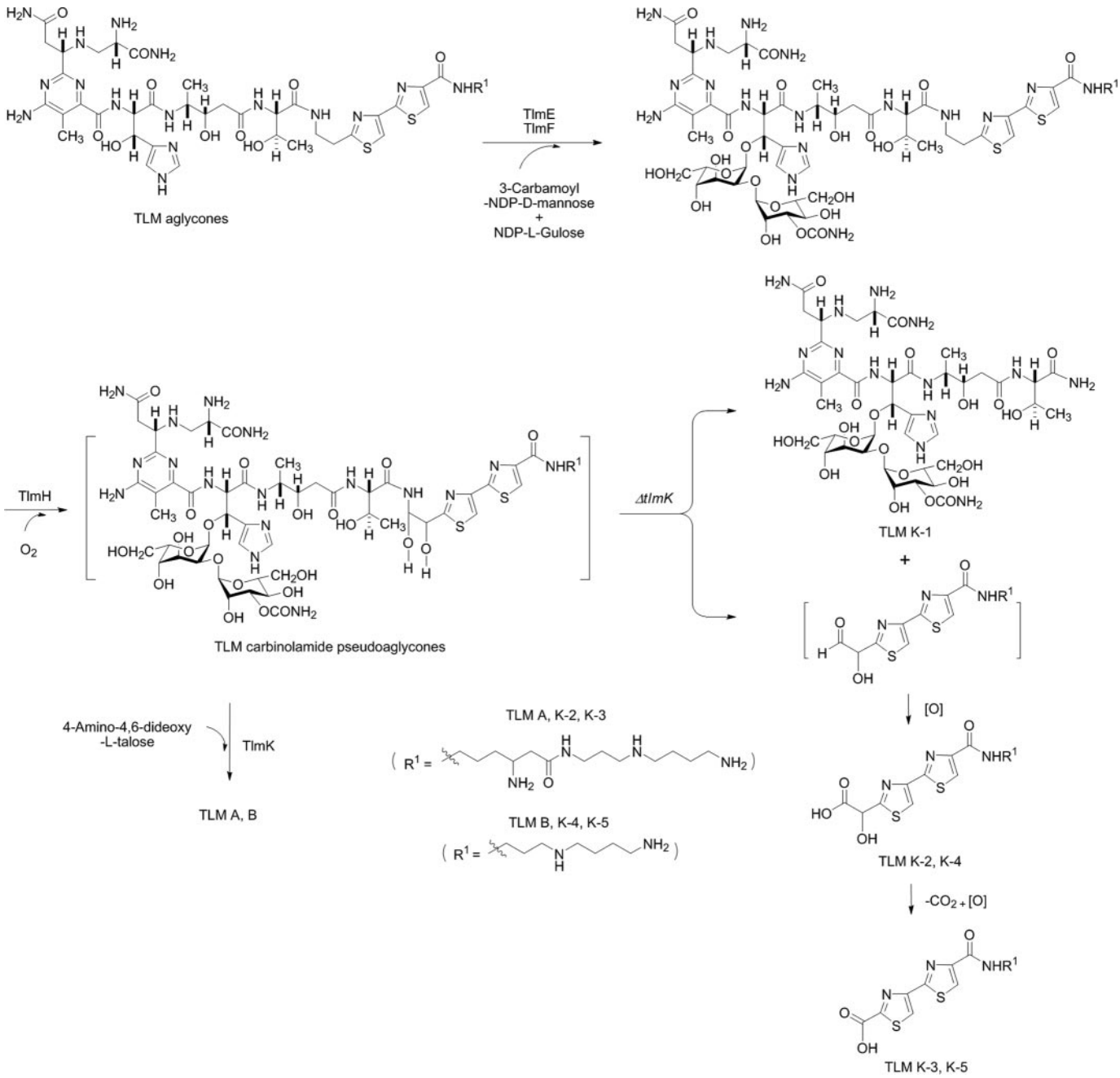

FIGURE 4. **Biosynthesis of TLMs featuring the carbinolamide pseudoaglycones as key intermediates, which in the absence of the TlmK glycosyltransferase, undergo rapid degradation into TLM K-1, K-2, K-3, K-4, and K-5.**

mediate single- and double-strand DNA cleavage at the 5′-GT or GC dinucleotide sites through an activated Fe(II)-complex form of BLM (3). Each structural unit of BLMs has been proved to contribute importantly to its biological activity through the extensive studies over the past 40 years (4, 5) (Fig. 1). The pyrimidoblamic acid and the linked β-hydroxyhistidine, defined as the metal binding domain, is involved in oxygen activation and radical generation, which are responsible for the final DNA cleavage. The role of the carbohydrate domain is known to enhance cleavage efficacy. Recent crystal structure of the DNA-Co-BLM complex suggested that the disaccharide serves as a space-filling unit and also by intermolecular hydrogen bonding interaction to enhance the binding of BLMs and DNA, thereby allowing the metal binding domain to adopt an optimized position to the target cleavage site (35). The C-terminal bithiazole moiety and positively charged amine tail serve as the DNA binding domain through an intercalation at the DNA recognition site. The linker region including the threonine and valerate moieties stabilizes the DNA binding with the BLMs through hydrogen-bonding between the hydroxyl group of the valerate moiety and the sugar phosphate backbone (3, 35).

To address the function of the metal chelating structural unit, the full metal binding domain of BLMs, including the pyrimidoblamic acid, β-hydroxyhistidine, and the disaccharide moiety, has been synthesized and was found to cleave super-

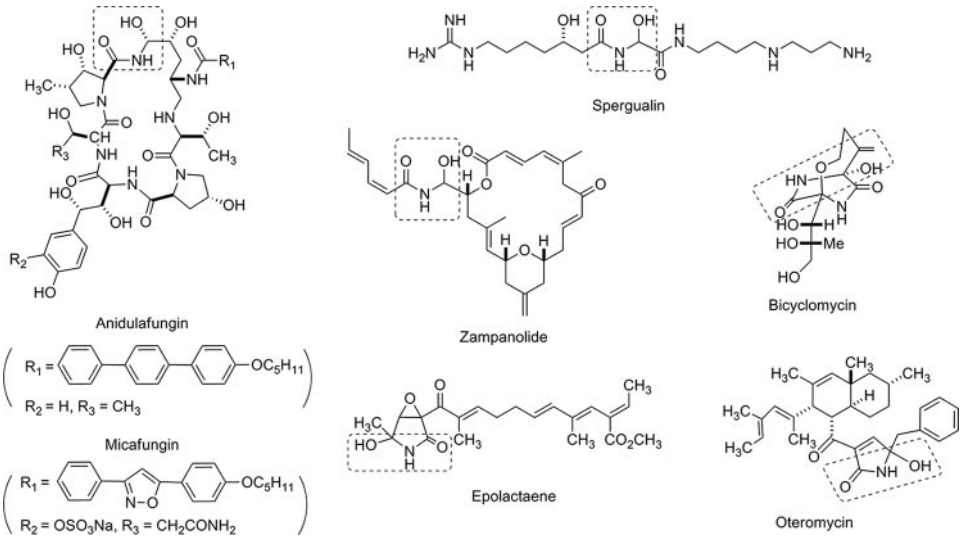

FIGURE 5. **Selected natural products containing a carbinolamide moiety (*boxed*).**

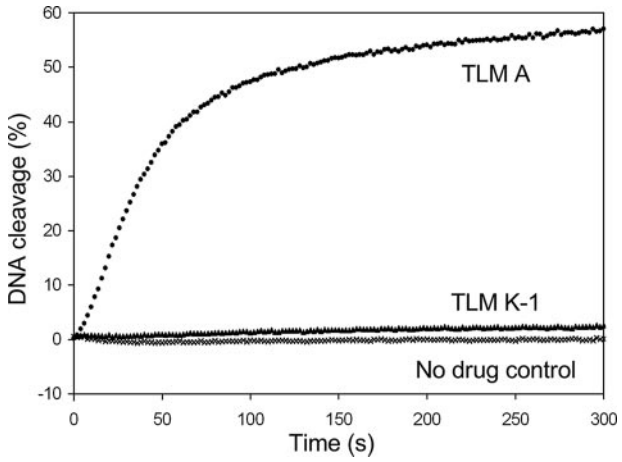

FIGURE 6. **Cleavage of the break light by TLM A, TLM K-1, and TLM K-2 assayed according to the literature procedure (39).** DNA cleavage was followed over time of assays containing 3.2 nM break light and TLM A (●, 200 nM), TLM K-1 (▲, 2 μM), TLM K-2 (2 μM, data not shown), or no drug as a control (×) in 25 mM Tris-HCl (pH 7.5) at 37 °C. TLM K-2, whose data were omitted from the plot for clarity, was identical to the no drug control.

coiled ΦX174 DNA in the presence of O_2 (Fe(II)) at 2–4-fold more effective than the background level (*i.e.* Fe(II) and O_2 alone) but 30–40-fold less effective than BLM A2 (36). In a more sensitive method using a ^{32}P 5′-end-labeled double-stand DNA w794 and its complement w836, the H_2O_2-Fe(III) complex of this compound was demonstrated to be 5–6-fold more effective than H_2O_2-Fe(III) alone but 200–300-fold less effective than BLM A2 (36). The metal binding domain lacking the disaccharide moiety failed to have any DNA cleavage activity above the background level (36). Bleomycinic acid, which only lacks of the terminal amine moiety compared with BLM A2, was only 35% effective on total DNA cleavage compared to that mediated by BLM A2 (37). The "extended" metal chelating unit, which includes the linker region, has not been synthesized yet and, thus, leaves us the question about the DNA cleavage activity of this key partial structure. The bithiazole DNA binding domain was also synthesized, and no DNA cleavage activity was found, although the chlorinated bithiazoles were found to effect potent light-mediated DNA cleavage via chlorine radicals (38).

In this study we generated the "left" and "right", two parts of the BLMs molecule by metabolic pathway engineering and product self-degradation. The left part, *i.e.* TLM K-1, includes the whole metal chelating domain, disaccharide, and the linker region, and the right part, *i.e.* TLM K-2, K-3, K-4, and K-5, consists of the bithiazole moiety and the terminal amines (Figs. 1 and 4). As we expected, the whole molecule of TLM A showed significant DNA cleavage activity in presence of Fe(II) and oxygen (Fig. 6). In contrast, TLM K-1 only showed limited activity right above the background cleavage, and TLM K-2 showed no activity even in high concentrations. The DNA cleavage velocity of TLM K-1 dropped by about 140 times compared with TLM A under the conditions examined. These results suggested that the metal binding domain of BLMs chelates a metal ion for oxygen activation and radical generation, which is required for DNA cleavage. But this domain, alone or combined with the linker domain, can only cleave DNA with minimal activity above the background level. The bithiazole and terminal amine part provides DNA recognition and intercalation moiety to facilitate DNA cleavage. Without the coordination of the whole molecule, each structure unit alone could not generate efficient bioactivity in DNA cleavage.

Supporting online information online includes experimental procedures for the detection of DNA cleavage activity of TLM A, K-1, and K-2 by break-light assay (39) and Tables S1 for plasmids, Tables S2 for bacterial strains, and Table S3 for oligonucleotides as PCR primers used in this study.

Acknowledgments—We thank the Analytical Instrumentation Center of the School of Pharmacy, University of Wisconsin-Madison for support in obtaining MS and NMR data and the John Innes Center, Norwich, UK, for providing the λ RED-mediated PCR-targeting mutagenesis kit.

REFERENCES

1. Kawaguchi, H., Tsukiura, H., Tomita, K., Konishi, M., and Saito, K. (1977) *J. Antibiot.* (*Tokyo*) **30,** 779–788
2. Konishi, M. S. K., Numata, K., Tsuno, T., and Asama, K. (1977) *J. Antibiot.* (*Tokyo*) **30,** 789–805
3. Chen, J., and Stubbe, J. (2005) *Nat. Rev. Cancer* **5,** 102–112
4. Hecht, S. M. (2000) *J. Nat. Prod.* **63,** 158–168
5. Boger, D. L., and Cai, H. (1999) *Angew. Chem. Int. Ed.* **38,** 448–476
6. Leitheiser, C. J., Smith, K. L., Rishel, M. J., Hashimoto, S., Konishi, K., Thomas, C. J., Li, C., McCormick, M. M., and Hecht, S. M. (2003) *J. Am. Chem. Soc.* **125,** 8218–8227
7. Shen, B., Du, L., Sanchez, C., Edwards, D. J., Chen, M., and Murrell, J. M. (2002) *J. Nat. Prod.* **65,** 422–431
8. Tao, M., Wang, L., Wendt-Pienkowski, E., George, N. P., Galm, U., Zhang, G., Coughlin, J. M., and Shen, B. (2007) *Mol. Biosyst..* **3,** 60–74
9. Galm, U., Wendt-Pienkowski, E., Wang, L., Geor-ge, N., Oh, J., Yi, F., Tao, M., Coughlin, J., and Shen, B. (2009) *Mol. Biosyst.* **5,** 77–90
10. Nicaise, C., Ajani, J., Goudeau, P., Rozencweig, M., Levin, B., and Krakoff,

I. (1990) *Cancer Chemother. Pharmacol.* **26,** 221–222
11. Nicaise, C., Hong, W. K., Dimery, W., Usakewicz, J., Rozencweig, M., and Krakoff, I. (1990) *Investig. New Drugs* **8,** 325–328
12. MacNeil, J., Gewain, M., Ruby, L., Dezeny, G., Gibbons, H., and MacNeil, T. (1992) *Gene* (*Amst.*) **111,** 61–68
13. Sambrook, J., and Russell, W. (2001) *Molecular Cloning*: *A Laboratory Manual*, 3rd Ed., Cold Spring Harbor Laboratory Press, Cold Spring Harbor, New York
14. Gust, B., Challis, L., Fowler, K., Kieser, T., and Chater, F. (2003) *Proc. Natl. Acad. Sci. U. S. A.* **100,** 1541–1546
15. Kieser, T., Bibb, J., Buttner, J., Chater, F., and Hopwood, A. (2000) *Practical Streptomyces Genetics*, 2nd Ed., John Innes Foundation, Norwich, UK
16. Bibb, M., White, J., Ward, J., and Janssen, J. (1994) *Mol. Microbiol.* **14,** 533–545
17. Greenaway, F. T., Dabrowiak, J. C., Grulich, R., and Crooke, S. T. (1980) *Org. Magnet. Res.* **13,** 270–273
18. Calafat, A., Won, H., and Marzilli, L. (1997) *J. Am. Chem. Soc.* **119,** 3656–3664
19. Miyaki, T., Numata, K., Matsumoto, K., Yamamoto, H., Nishiyama, Y., Ohbayashi, M., Imanishi, H., Konishi, M., and Kawaguchi, H. (1981) *J. Antibiot.* (*Tokyo*) **34,** 658–664
20. Fujii, A., Takita, T., Shimada, N., and Umezawa, H. (1974) *J. Antibiot.* (*Tokyo*) **27,** 73–77
21. Oka, S. (1980) *Recent Res. Cancer Res.* **74,** 163–171
22. Mansouri, K., and Piepersberg, W. (1991) *Mol. Gen. Genet.* **228,** 459–469
23. Debono, M., Turner, W. W., LaGrandeur, L., Burkhardt, F. J., Nissen, J. S., Nichols, K. K., Rodriguez, M. J., Zweifel, M. J., Zeckner, D. J., and Gordee, R. S. (1995) *J. Med. Chem.* **38,** 3271–3281
24. Tawara, S., Ikeda, F., Maki, K., Morishita, Y., Otomo, K., Teratani, N., Goto, T., Tomishima, M., Ohki, H., Yamada, A., Kawabata, K., Takasugi, H., Sakane, K., Tanaka, H., Matsumoto, F., and Kuwahara, S. (2000) *Antimicrob. Agents Chemother.* **44,** 57–62
25. Umezawa, H., Kondo, S., Iinuma, H., Kunimoto, S., Ikeda, Y., Iwasawa, H., Ikeda, D., and Takeuchi, T. (1981) *J. Antibiot.* (*Tokyo*) **34,** 1622–1624
26. Smith, A., Safnov, I., and Corbett, R. (2002) *J. Am. Chem. Soc.* **124,** 11102–11113
27. Kamiya, T., Maeno, S., Hashimoto, M., and Mine, Y. (1972) *J. Antibiot.* (*Tokyo*) **25,** 576–581
28. Miyoshi, T., Miyairi, N., Aoki, H., Kosaka, M., and Sakai, H. (1972) *J. Antibiot.* (*Tokyo*) **25,** 569–575
29. Miyamura, S., Ogasawara, N., Otsuka, H., Niwayama, S., and Tanaka, H. (1973) *J. Antibiot.* (*Tokyo*) **26,** 479–484
30. Kakeya, H., Takahashi, I., Okada, G., Isono, K., and Osada, H. (1995) *J. Antibiot.* (*Tokyo*) **48,** 733–735
31. Singh, S., Goetz, M., Jones, E., Bills, G., Giacobbe, R., Herranz, L., Miles, S., and Williams, D. (1995) *J. Org. Chem.* **60,** 7040–7042
32. James, D., Martin, S., David, K., Timothy, H., and Irving, W. (2005) *J. Clin. Pharmacol.* **45,** 227–233
33. Dowell, J., Pu, F., LEE, J., Stogniew, M., Krause, D., and Henkel, T. (2003) *Interscience Conference of Antimicrobiology Agents and Chemotherapy*, *Chicago*, *September 14, 2003*, Abstr. A-1576, American Society for Microbiology
34. Troast, D., and Porco, J. (2002) *Org. Lett.* **4,** 991–994
35. Goodwin, K., Lewis, M., Long, C., and Georgiadis, M. (2008) *Proc. Natl. Acad. Sci. U. S. A.* **105,** 5052–5056
36. Boger, D. L., Teramoto, S., Honda, T., and Zhou, J. (1995) *J. Am. Chem. Soc.* **117,** 7338–7343
37. Shipley, B., and Hecht, M. (1998) *Chem. Res. Toxicol.* **1,** 25–27
38. Zuber, G., Quada, J., and Hecht, M. (1998) *J. Am. Chem. Soc.* **120,** 9368–9369
39. Biggins, J. B., Prudent, J. R., Marshall, D. J., Ruppen, M., and Thorson, J. S. (2000) *Proc. Natl. Acad. Sci. U. S. A.* **97,** 13537–13542